

# Design and Implementation of Time-Sensitive Wireless IoT Networks on Software-Defined Radio

Jiaxin Liang, He Chen, *Member, IEEE*, and Soung Chang Liew, *Fellow, IEEE*

**Abstract**—Time-sensitive wireless networks are important enabling building blocks for many emerging industrial Internet of Things (IoT) applications. Quick prototyping and evaluation of time-sensitive wireless technologies are becoming increasingly important. Software defined radio (SDR), which enables wireless signal processing on a personal computer (PC), has been widely used for such quick prototyping efforts. However, because of the *uncontrollable latency* between the PC and the radio board, SDR is generally deemed not suitable for time-sensitive wireless applications that demand communication with low and deterministic latency. For a rigorous evaluation of its suitability for industrial IoT applications, this paper conducts a quantitative investigation of the synchronization accuracy and end-to-end latency achievable by an SDR wireless system. To this end, we designed and implemented a time-slotted wireless system on the Universal Software Radio Peripheral (USRP) SDR platform. To address the latency challenge, we developed a time synchronization mechanism to maintain synchrony among nodes in the system. To reduce the latency and to handle the delay jitter between the USRP board and its PC, we devised a *Wake-ahead-a-bit* algorithm to ensure that packets sent by the PC to the USRP can reach the USRP just before the time slots they are to be transmitted. Our experiments demonstrate that 90% (100%) of the time slots of different nodes can be synchronized and aligned to within  $\pm 0.5$  samples or  $\pm 0.05\mu s$  ( $\pm 1.5$  samples or  $\pm 0.15\mu s$ ), and that the end-to-end packet delivery latency can be down to  $3.75ms$ . This means that SDR-based solutions can be applied in a range of IIoT applications that require tight synchrony and moderately low latency, e.g., sensor data collection, automated guided vehicle (AGV) control, and Human-Machine-Interaction (HMI) [1], [2].

**Index Terms**—Time-sensitive wireless networks, industrial IoT, time-slotted system, time synchronization, software-defined radio.

## I. INTRODUCTION

The industrial Internet of Things (IIoT), which generally refers to as the applications of IoT technologies in the industrial domain, has attracted tremendous attention from governments, academia, and industry, thanks to its potential to boost the flexibility and efficiency of future smart factories [3]. As pointed out by the industry giant GE, providing powerful and pervasive connectivity between machines, workers and materials in factories will be essential to unlocking the full potential of IIoT [4].

Connectivity between devices in an industrial environment has until now been dominated by wired communication. Replacing the wired communication infrastructure in today's factories by its wireless counterpart will bring many benefits, including reduced installation and maintenance costs, quick

reconfiguration, and mobility [5], [6]. However, simple installation of current wireless technologies like WiFi and 4G in the industrial environment will not bring satisfactory performance [7]. Typical industrial applications require deterministic real-time exchange of small amounts of data (e.g., a single control command) with tight delay constraints, whereas modern wireless communication systems have been engineered for the exchange of large amounts of data with loose requirements on synchrony and timeliness [8]. To close this gap, conventional solutions that rely on general-purpose wireless chipsets may need to be replaced with dedicated solutions [6] with customized wireless physical and data-link layer designs tailored for time-sensitive industrial applications.

Software-defined radio (SDR), widely studied in the past few decades, are appealing alternatives to conventional radio, thanks to its modularity and lower development costs [6], [9]. The main goal of SDR is to facilitate the implementation of radio signal processing components, traditionally done on customized hardware (e.g., equalizers, modulators, and coders), by software on general-purpose computing platforms like PCs. The softwarization can significantly shorten the development and evaluation cycle of new radio techniques.

Existing development efforts on SDR platforms have focused on consumer wireless technologies (e.g., IEEE 802.15.4 [10], IEEE 802.11a [11], [12], IEEE 802.11ac MIMO [13], and standard encoder/decoder modules [14]). Due to the indeterminate delays in the SDR architecture (e.g., processing delay in the PC, and transmission delay between the PC and the radio board, are random), the "PC + radio board" SDR structure has been widely deemed not suitable for time-sensitive IIoT applications. However, there has been no quantitative evaluation to quantify the extent to which this impression is true i.e., there are no systematic study on the range of deterministic delays achievable by the "PC + radio board" SDR architecture.

For time-critical applications, a new model-based SDR approach has been introduced, where software tools are used to automatically translate high-level models to low-level hardware description language (HDL) [6]. These tools enable the replacement of the general-purpose PC by the Field-programmable gate array (FPGA) embedded systems for fast signal processing. Though the original goal of the model-based SDR is to allow designers to focus on system-level designs only, efficient implementation and debugging of the designs still demand a deep understanding of FPGA and its programming. Model-based SDR is much harder to handle than PC-based SDR, especially for people with software programming background only.

Meanwhile, a new trend, initiated by the O-RAN Alliance made up of major worldwide mobile operators and computing

J. Liang, H. Chen, and S. C. Liew are with Department of Information Engineering, The Chinese University of Hong Kong, Hong Kong SAR, China (email: {lj015, he.chen, soung}@ie.cuhk.edu.hk).

platform manufactures, is to develop commercial radio-access unit (RAN) products based on a “PC + radio board” architecture similar to PC-based SDR [15]. For real-time performance, the O-RAN Alliance promotes the use of powerful computing platforms and real-time operating systems (OS).

This new trend motivates us to revisit an unanswered question: How to efficiently enhance the performance of the PC-based SDR, in terms of its synchronization precision and end-to-end latency, to allow it to support time-sensitive IIoT applications? To answer this question, we designed and implemented a real-time time-slotted wireless system on the Universal Software Radio Peripheral (USRP) SDR radio platform connected to general-purpose PCs running non-real-time OS. We refer to our system as RTTS-SDR (Real-Time Time-slotted System over SDR).

There are two fundamental challenges to the design of RTTS-SDR. The first challenge is the time synchronization challenge: to align the time slot boundaries of different nodes without the nodes being physically connected to a common external clock source, subject to the random delays between the USRP and the PC of the nodes. The second challenge is the low-latency challenge: to ensure the USRP of a node will transmit a packet in a near-future time slot specified by its PC, again subject to the random delay between the PC (where the samples and instructions are generated) and the USRP (where the samples are transmitted).

RTTS-SDR has several salient features: (1) It incorporates a time-synchronization mechanism to maintain microsecond-level synchrony among nodes. (2) It uses a “Wake-ahead-a-bit” algorithm to ensure that, at the transmitter side, the PC generates and sends a packet to the USRP just a little ahead of the transmission time of the packet at the USRP, thereby reducing the end-to-end delivery latency. (3) It is a complete TCP/IP compatible system ready to run any TCP/IP application. (4) It can be reconfigured for different latency-throughput requirements by changing PHY and data-link layer parameters.

We note that [16] designed and implemented a customized PHY layer on the USRP platform. However, the implementation involves offline rather than real-time signal processing and is therefore not ready to run real applications. [17] proposed a beacon-based synchronization method to synchronize the nodes in an IEEE 802.15.4 based cluster-tree network. However, [17] mainly focused on the scalability and the overhead of the algorithm, with the precision of the synchronization being largely overlooked. RTTS-SDR, on the other hand, employs a beacon-based synchronization to achieve microsecond-level synchrony with moderately low latency. Importantly, real-time applications can run on top of RTTS-SDR, thanks to real-time signal processing and other essential protocol-stack implementations. Recently, several work in the IIoT field [18], [19] also leverages the PC-based SDR to prove their new system designs.

Experiments on RTTS-SDR demonstrate that 90% (100%) of the slot boundaries of different nodes can be synchronized to within  $\pm 0.5$  samples or  $\pm 0.05\mu s$  ( $\pm 1.5$  samples or  $\pm 0.15\mu s$ ), and that packets of length 36 bytes can be delivered with deterministic end-to-end delay down to  $3.75ms$ . RTTS-

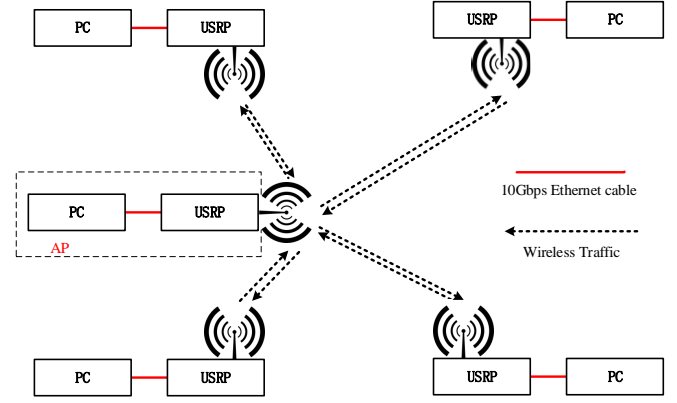


Fig. 1. An example of a 5-node system. One of the nodes serves as the AP and other nodes serve as the IIoT devices. The AP is responsible for synchronization.

SDR currently runs on a generic Linux OS—we believe that the latency can be further reduced if it is deployed on a real-time OS.

## II. SYSTEM ARCHITECTURE

This section provides an overview of the system architecture and the problems addressed by this paper.

### A. System architecture

Fig. 1 shows an example with 5 nodes. Each node consists of a PC and a USRP interconnected by a 10Gbps Ethernet cable. One of the nodes is the AP, which is also the synchronization coordinator of the overall system. The other nodes are IIoT devices. Specifically, the AP’s USRP clock gives the system’s global reference time. We use  $i$  to represent the index of a node. The AP has index 0 (i.e.  $i = 0$ ).

RTTS-SDR provides the functionalities of the Physical (PHY) layer, the Data link layer, and the Network layer. Fig. 2 shows the communication through the layers between two nodes. Users run applications (APP layer) over the TCP/IP layer. The TCP/IP layer then puts the data into or extract the data from the LLC layer and the layers below. RTTS-SDR provides the orange blocks (LLC, MAC, and PHY) that are fully compatible with the existing TCP/IP layer in the OS.

To ensure TCP/IP compatibility, we use the TAP device [20] in the OS as a virtual network card to interact with the TCP/IP layer. For the TX path, when an IP datagram is forwarded to the virtual network card, the TAP device generates an Ethernet frame with the IP datagram as the payload and forwards the Ethernet frame to the program that created the TAP device. GNURadio is the program that creates the TAP device in our system. GNURadio then generates the baseband samples based on the content of the Ethernet frame and sends them to the USRP. For the RX path, GNURadio processes the baseband samples coming from the USRP and then forwards the processed data to the TAP device.

The MAC layer in our system adopts a time-slotted medium access scheme. Due to the random delay jitters between the PC and the USRP, timing control is challenging in the time-slotted

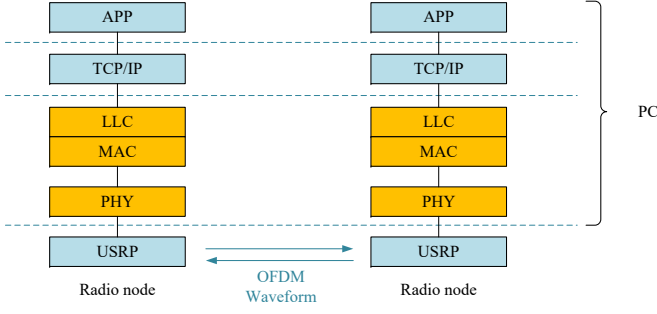


Fig. 2. RTTS-SDR provides the complete design for the orange blocks, i.e., LLC, MAC, and PHY.

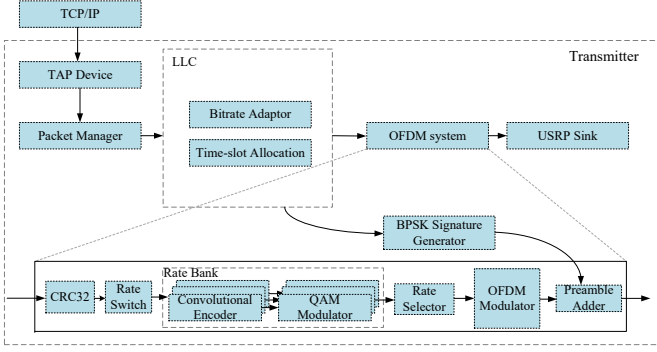


Fig. 3. Transmitted-side PHY Design.

system. In particular, when the PC instructs the USRP to transmit a particular frame in a certain time slot, the PC must ensure this frame will arrive at the USRP and be processed at the USRP before the time slot.

Fig. 3 shows the diagram of the PHY layer at the transmitter side. The Ethernet frame from TAP is first passed to a packet manager responsible for Logical Link Control (LLC) and MAC-layer operations. It computes and generates information related to rate decision, synchronization, and packet queueing. The computed results and decisions are put in tags<sup>1</sup> padded along with the information bits, which are then forwarded to an OFDM system. A block, called Rate Bank, contains a bank of convolutional encoders and QAM modulators to provide bitrate variation support. Each set of a convolutional encoder and a QAM modulator gives one rate. After the QAM modulation, the symbols are then put into an OFDM modulator which performs subcarrier mapping and IFFT operations. Finally, a preamble is prepended to the packet. At the receiver side, a reverse process is performed on the received samples, as shown in Fig. 4.

### B. Problem description

RTTS-SDR is a time-slotted system which divides the channel resources into multiple time slots (see Fig. 5). Before

<sup>1</sup>Tag, also known as Stream Tag [21], is a mechanism in GNUradio to pass control information between blocks. Several tags can piggyback on each baseband sample. GNUradio also uses Tag to control hardware. When the samples with hardware-control tags arrive at the UHD (the USRP Hardware Driver [22]), the UHD configures the USRP hardware according to the tag instructions.

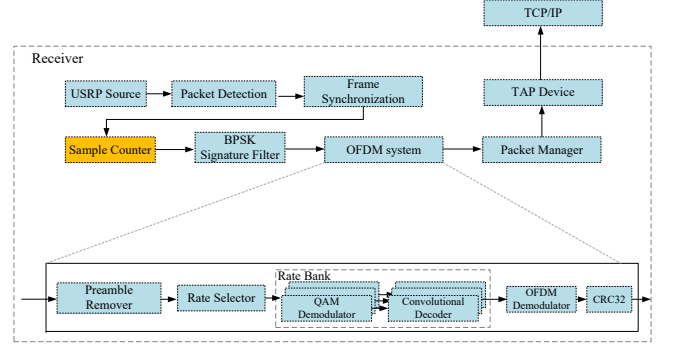


Fig. 4. Receiver-side PHY Design.

delving into the details, let us first define some notations to ease explanation. We use the upper-case  $T$  to denote the time counter variable at a node. A particular value sampled from the time counter is denoted by a lower-case  $t$ . For example, by  $T = t$ , we mean the value associated with time variable  $T$  is  $t$  at a particular moment in time.

Three types of local times can be kept at a node: (i) USRP time, (ii) PC time, and (iii) USRP time on PC.

**USRP time** refers to the time maintained by the time counter on the USRP. USRP time increments according to the local oscillator within the USRP. We denote the USRP time variable of node  $i$  by  $T_{U,i}$  and the USRP time value by  $t_{U,i}$ . USRP time is purely a hardware time. It is used, for example, to time the transmission of packets by the RF board. For a node  $i$ , a packet is said to be transmitted at time  $t_E$  (or with timestamp  $t_E$ ) if it is transmitted when the USRP time variable  $T_{U,i} = t_E$ .

**PC time** is the time maintained by the PC's OS. PC time can be obtained by calling the function `time.time()` within a program. We denote the PC time variable (value) in node  $i$ 's PC by  $T_{P,i}$  ( $t_{P,i}$ ).

**USRP time on PC** is the USRP time known by the connected PC and it is denoted by  $T_{UP,i}$  ( $t_{UP,i}$  for a value) for node  $i$ . Every time a program on the PC tries to get<sup>2</sup> the *USRP time* through UHD, UHD will instruct the USRP to capture the current USRP time  $T_{U,i} = t_{U,i}$  and send that time to the PC. The actual USRP time is always larger than the USRP time on PC. Denote the delay<sup>3</sup> between USRP and PC at node  $i$  by  $\delta_i$ , we have

$$T_{U,i} = T_{UP,i} + \delta_i \quad (1)$$

For the time-slotted mechanism, let  $s_j^k$  be the *global time* slot boundaries for slot  $j$  of the  $k$ -th frame and  $s_{i,j}^k$  be the time at which **node  $i$  thinks** slot  $j$  of the  $k$ -th frame begins (also known as time slot boundary), i.e.,  $s_{i,j}^k$  is the transmission time for a packet to be transmitted in time slot  $j$  of the  $k$ -th frame by node  $i$ . If the first sample of a packet is tagged with a timestamp  $s_{i,j}^k$ , it will be transmitted by node  $i$ 's USRP when

<sup>2</sup>UHD provides a function `get_usrp_hardware_time()` for the PC to get the USRP time.

<sup>3</sup>The overall delay between USRP and PC includes the PC command processing time, delay caused by Ethernet packet transmission and USRP command response time. According to our experience, the overall delay is typically dominated by the Ethernet packet delivery delay.

$T_{U,i} = s_{i,j}^k$ . In our system, the AP's USRP time is regarded as the global reference time, that is,  $s_j^k = s_{0,j}^k$ . Meanwhile, the time that node  $i$  receives a packet from another node in slot  $j$  in  $k$ -th frame is denoted by  $\tilde{s}_{i,j}^k$ .

For the considered time-slotted system, the boundaries of time slots maintained by different nodes need to be aligned so as to synchronize the access of the wireless medium. As such, we are required to design a synchronization mechanism tailored for the SDR platform. Our synchronization mechanism design faces two challenges: The first challenge is to align the slot boundaries of the nodes (i.e.,  $s_{i,j}^k$ ), subject to the random delays between the USRP and the PC of the nodes, different propagation delays between different pairs of nodes, and different local clock shifts. The second challenge is to ensure the USRP of a node transmits a packet precisely in a near-future time slot specified by its PC, again subject to the random delay between the PC (where the samples and instructions are generated) and the USRP (where the samples are transmitted).

To address the first challenge, we adopt a beacon synchronization and sample counting mechanism, as elaborated in Section III. To address the second challenge, we propose an algorithm called “Wake-ahead-a-bit” to ensure that packets sent out by the PC to the USRP can reach the USRP before the time slots they are to be transmitted, which will be presented in Section IV.

### III. TIME SYNCHRONIZATION

In RTTS-SDR, different nodes have different USRP time and PC time. To synchronize their time and align their time slot boundaries, a mechanism for the exchange of time information is needed so that they can reach a consensus on the time slot boundaries. We put forth a new mechanism tailored for SDR called beacon synchronization.

The misalignment of the slot boundaries of different nodes is mainly caused by the following problems: (1) different nodes use different USRP clocks to time packet transmission and reception; (2) random delays between PC and USRP; (3) different propagation delays and clock offsets among different pairs of nodes.

Our approach to solving the above problems to synchronize the slot boundaries of different nodes include: (1) a beacon synchronization mechanism to let all the IoT devices obtain information on the global reference time (i.e., AP's USRP Time), as presented in Section III-A; (2) a sample counting algorithm for a node to acquire the precise packet arrival time, as presented in Section III-B; (3) a modified version of the Precision Time Protocol (PTP) to compensate for the propagation delays and clock offsets between AP and IoT devices, as presented in Section III-C. Section III-D discusses the implications of beacon transmission loss. Section III-E presents our algorithm for detecting the starting point of a packet. Finally, Section III-F explains how to leverage the accurate synchronization among the USRPs to provide an *Event Synchronization* service to applications.

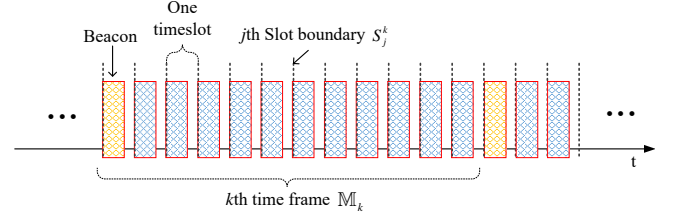


Fig. 5. In RTTS-SDR, the channel resource is divided into slots and  $N$  slots are grouped into a time frame.

#### A. Beacon synchronization

1) *Beacons as a time reference*: As shown in Fig. 5, our time-slotted system divides the channel resources into multiple time slots. A group of  $N$  time slots forms a time frame. The first time slot in a time frame is dedicated to the transmission of a beacon by the AP. Beacons, commonly used to broadcast control information and feedback information, also serves as a reference packet providing timing to align the slot boundaries of the other nodes. The transmission of the beacon is timed according to the AP's USRP clock.

2) *Two phases of synchronization*: The beacon synchronization mechanism in our system is divided into two phases: (1) beacon broadcast phase by the AP and (2) slot alignment phase by IoT devices.

In the **beacon broadcast phase**, a beacon for the  $k$ -th frame is first generated at the AP's PC. The AP's PC tags the beacon with a USRP transmission timestamp  $s_{0,0}^k$  and then sends the beacon to the AP's USRP, which transmits it when  $T_{U,0} = s_{0,0}^k$ , where  $T_{U,0}$  is the AP's USRP time. We emphasize that the PC needs to send the beacon to the USRP ahead of  $T_{U,0} = s_{0,0}^k$  due to the random delays between them. Details will be discussed in Section IV.

In the **slot alignment phase**, upon receiving the beacon, an IoT device adjusts its slot boundaries to align with the slot boundaries of the AP. Specifically, an IoT device  $i$  records the beacon's arrival time according to its own USRP timer,  $T_{U,i} = \tilde{s}_{i,0}^k$ . The IoT device  $i$  then computes the times of its subsequent slot boundaries,  $s_{i,j}^l$ ,  $j > 0, l \geq k$ , based on  $\tilde{s}_{i,0}^k$ , as elaborated below.

3) *Time slot boundary computation*: For a frame of size  $N$ , there are  $N - 1$  time slots following the beacon. Since we have the arrival time of the beacon  $\tilde{s}_{i,0}^k$  in the  $k$ -th time frame, we can compute the time of the  $j$ -th time slot boundary in the  $l$ -th time frame  $s_{i,j}^l$  by

$$s_{i,j}^l = \tilde{s}_{i,0}^k + (l - k)NT_s + jT_s, \quad (2)$$

where  $T_s$  is the duration of a time slot (i.e., the gap between two consecutive time slot boundaries). Eq. (2) shows that one can compute all the times of the slot boundaries following the beacon. We will shortly show in Section V-B that, due to the clock drifts between the AP and the IoT devices (i.e., the clocks at different nodes may tick at slightly different rates), the slot boundary times computed by (2) are no longer reliable after a few frames. Resynchronization based on a new beacon is necessary. In addition, (2) has not taken the propagation delays between the AP and the IoT device into account. To do so, it will be replaced by (9) later.



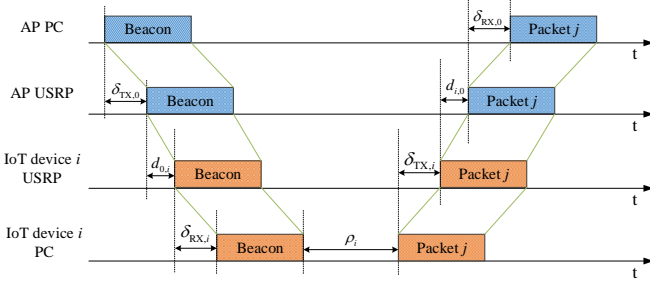


Fig. 6. An example showing how delays affect the transmission and reception of beacons/packets. When the AP's PC sends a beacon, it takes  $\delta_{TX,0}$  amount of time for it to arrive at the AP's USRP. If the USRP transmits the beacon immediately, then after  $d_{0,i}$  propagation delay, the beacon arrives at node  $i$ 's USRP. The USRP then sends the beacon to the PC, incurring an additional  $\delta_{RX,i}$  delay. The PC takes  $\rho_i$  amount of time to process the samples and prepare packet  $j$ .  $\delta_{TX,i}$  is the TX delay for the IoT device  $i$  and  $\delta_{RX,0}$  is the RX delays for the AP.

Although the idea of a two-phase synchronization mechanism seems straightforward, implementing the mechanism on the SDR platform is not trivial. In particular, it is not straightforward for the PC to acquire the exact arrival time of the beacon on its associated USRP due to the random delays between them. The beacon arrival time is essential for the GNURadio running on the PC to execute the slot boundary alignment. A simple method is to get the *USRP Time* only after the beacon is decoded by the PC. However, *USRP Time on PC* is always outdated (as shown in (1)). Next, we elaborate on our approach for the precise acquisition of the beacon arrival time.

### B. Acquisition of precise arrival time

To acquire the precise beacon arrival time, we need to circumvent the effects of the inter USRP-PC delay and the PC beacon decoding delay. It turns out that although the USRP does not provide the arrival time of a packet or a sample directly, it gives the timestamp  $t_{init}$  of the USRP counter when its RX path is first started up by the PC during the initialization stage. This timestamp is then piggybacked on the first received sample in the RX path and sent to the PC. In other words, the PC has the *USRP time* when the first sample is received on the RX path. We can derive the *USRP time* of the later samples by a sample counting process, as elaborated below.

In our system, the bandwidth is  $B$ , and thus the duration of one sample  $T_{sample}$  is equal to  $1/B$ . As shown in Fig. 4, we add a block called **Sample Counter** after the Frame synchronization block. When the USRP receiver outputs new samples (Note that the USRP receiver samples signal from the air channel continuously without interruption), the *Sample Counter* counts the number of incoming samples. Once the Frame synchronization block detects a peak signifying the beginning of a beacon, it will put a special tag at the sample corresponding to the beginning of the packet. The *Sample Counter*, upon detecting the special tag associated with the sample, can then compute the sample's *USRP Time* by

$$t_b = t_{init} + K \cdot T_{sample}, \quad (3)$$

<sup>3</sup>We omit the USRP hardware's circuit time in this example.

where  $K$  is the number of passed samples the *Sample Counter* has counted.  $t_b$  is taken as the slot boundary indicated by the beacon, and it is put into a special tag so that other parts of the PC program can access it.

The expression in (2) is the boundary of a time slot computed based on the beacon received at the receiver of node  $i$ . In general, different nodes will have different slot boundaries because of the different propagation delays from the AP to the IoT devices. Also, the packets transmitted by them to the AP may incur different propagation delays. Our goal is to synchronize and align the slot boundaries of different devices as perceived by the receiver of the AP. Toward that end, we will first need to estimate the propagation delay. The propagation delay can be estimated by applying a modified version of the PTP [23].

### C. Propagation delay and clock offset estimation

Let  $o_i$  be the clock offset between the AP's USRP clock and an IoT device  $i$ 's USRP clock,  $d_{0,i}$  be the propagation delay from the AP to the IoT device  $i$ , and  $d_{i,0}$  be the propagation delay in the opposite direction. Suppose the AP sends the  $k$ -th beacon at its USRP time  $T_{U,0} = s_{0,0}^k$ . The AP records that time into the beacon's payload as timing information to convey the IoT devices. When the beacon is transmitted at  $T_{U,0} = s_{0,0}^k$ , the USRP time at the IoT device  $i$  is  $T_{U,i} = s_{0,0}^k + o_i$ . When the beacon arrives at the IoT device's receiver side (event 1), the USRP time of the IoT device is

$$t_i^{(1)} = \tilde{s}_{i,0}^k = s_{0,0}^k + o_i + d_{0,i}. \quad (4)$$

At this moment, the USRP time of the AP is  $t_0^{(1)} = s_{0,0}^k + d_{0,i}$ . Note that the IoT device  $i$  can retrieve the beacon transmission time  $s_{0,0}^k$  at the AP from the beacon payload, and it can obtain the value of  $t_i^{(1)}$  according to its own USRP clock,  $T_{U,i}$ . To the IoT device  $i$ , the unknowns in (4) at this point are  $d_{0,i}$  and  $o_i$ , which are to be estimated.

In a near-future time slot  $j$  of frame  $l$  allocated to the IoT device  $i$ , the IoT device  $i$  sends a data packet at its USRP time  $s_{i,j}^l$ , and  $s_{i,j}^l$  is recorded into the payload of the packet. When the AP receives the corresponding data packet (event 2), its USRP time is

$$t_0^{(2)} = s_{i,j}^l + d_{i,0} - o_i. \quad (5)$$

At this moment, the USRP time of the IoT device  $i$  is  $t_i^{(2)} = s_{i,j}^l + d_{i,c}$ . In the next transmitted beacon, the AP embeds  $t_0^{(2)}$  into the beacon's payload. By the time the IoT device receives the new beacon, it knows four values:  $t_i^{(1)}$ ,  $s_{0,0}^k$ ,  $s_{i,j}^l$ ,  $t_0^{(2)}$ . Therefore, it can estimate the propagation delay  $d_{0,i}$  by combining (4) and (5):

$$d_{0,i} = d_{i,0} = \frac{1}{2} \left( t_i^{(1)} + t_0^{(2)} - s_{0,0}^k - s_{i,j}^l \right), \quad (6)$$

$$o_i = \frac{1}{2} \left( t_i^{(1)} - t_0^{(2)} - s_{0,0}^k + s_{i,j}^l \right), \quad (7)$$

assuming that the propagation delays of both directions are the same (i.e.  $d_{0,i} = d_{i,0}$ ) and the clock offset  $o_i$  is constant. In Section V-B we will show that the clock offset  $o_i$  remains constant for a duration that is much longer than one frame

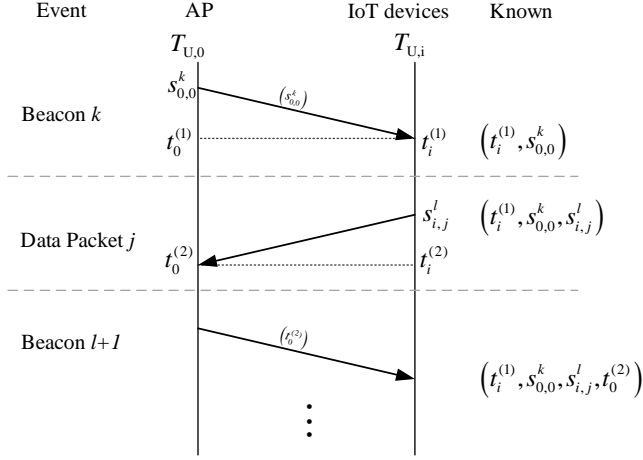


Fig. 7. A three-way handshake scheme based on PTP for both clock offset compensation and propagation delay compensation.

duration. A diagram in Fig. 7 shows the exchange and the acquisition of the timing information between the AP and the IoT device  $i$ .

The relationship between  $s_{0,0}^k$  and  $\tilde{s}_{i,0}^k$  can be written as

$$\tilde{s}_{i,0}^k = s_{0,0}^k + d_{0,i} + o_i. \quad (8)$$

Since the propagation delay is well estimated, to align the arrival of packets transmitted by different IoT devices at the AP, the transmission time of a packet for the  $j$ -th time slot in  $l$ -th time frame of the IoT device  $i$  should be set to

$$s_{i,j}^l = \tilde{s}_{i,0}^k + (l - k)NT_s + jT_s - 2d_{0,i}. \quad (9)$$

Note that (9) is different from (2) in that it lets the IoT device transmit its packet  $2d_{0,i}$  (i.e. round trip delay) earlier. If all IoT devices do this, then the transmission boundaries of the AP and the reception boundaries associated with all IoT devices align at the AP.

#### D. What if beacons are lost?

If a beacon is not detected due to noise or interference, the IoT device's future slot boundaries are not updated. A missed beacon, however, is not a big concern because of the high accuracy of the USRP oscillators (2.5 ppm). The slots of different nodes will not drift apart by more than a sample if the beacons of a small number of consecutive frames are missed.

#### E. Packet detection

As discussed in Section III-A2, to find the precise arrival time of the beacon/packet, the *Frame Synchronization* block must be able to find the first sample of a beacon correctly. Packet detection (finding the beginning of a packet from a train of received samples) is a common issue in asynchronous wireless communication networks in which nodes can generate and transmit packets at arbitrary times. There are two reasons why we still need packet detection in our synchronous time-slotted system: (i) our OFDM system is modified from that of a WiFi system, which is asynchronous in operation; (ii) finding

the positions of beacons is still important for the purpose of slot alignment even if we do not use *Frame Synchronization* to detect regular packets.

There are many methods for packet detection. Our method is based on a modification of the method in [24]. We refer the interested readers to Sections 2.2 and 2.4 of [24] for details. We modified the detection algorithm to provide the index of the first sample of a packet and piggyback a special tag on that sample. The Sample Counter block can then extract the special tag and determine the time of the  $j$ -th time slot boundary by

$$s_{i,j}^k = t_{\text{init}} + I_{\text{start}} \cdot T_{\text{sample}} + (l - k)NT_s + jT_s - 2d_{0,i}, \quad (10)$$

where  $l \geq k$  and  $I_{\text{start}}$  is the index of the first sample of the beacon received by the IoT device  $i$  in the  $k$ -th frame.

#### F. Implications of synchronized USRP times

By synchronizing the time-slot boundaries among the AP and the IoT devices, one can further synchronize the USRP times among the nodes. Specifically, the offsets between the AP's USRP clock and the IoT device  $i$ 's USRP clock  $o_i$  are obtained in (7) at the IoT device  $i$ , and the IoT device  $i$  can compute an estimate of the time of AP's USRP clock  $\hat{T}_{U,0,i}$  by

$$\hat{T}_{U,0,i} = T_{U,i} + o_i. \quad (11)$$

By having the precise time of the global clock in every IoT device, a service that relies on the timing information of the global clock can be provided to other applications besides just our time-slot alignment application, with the global time being the AP time. We name the service as **Event Synchronization**. For example, if we want different IoT devices to perform synchronized actions at a particular point in time, this service can be used to make sure these actions are indeed performed according to a common sense of time.

Based on this service, applications that require microsecond-level synchronization can now be handled. For an event  $E$  to happen at global time  $t_E$  at the IoT device  $i$  can be scheduled to happen at local time  $T_{U,i} = t_E + o_i$ . For example, if the IoT devices are sensors, we could coordinate them to make a measurement at exactly the global time  $t_E$  in a synchronized manner.

### IV. LOW LATENCY TRANSMISSION

This section develops a packet transmission scheme, named “Wake-ahead-a-bit”, to reduce delays in packet transmission.

The preparation of a packet to be transmitted consists of two steps: (1) preparation of the baseband samples; (2) preparation of the USRP timestamp for the first baseband sample's tag. Recall that a packet to be transmitted at *USRP Time*  $t_E$  needs to be tagged with a timestamp  $t_E$ . When a packet with a timestamp  $t_E$  is sent to the USRP, it will be put in a *SampleQueue* [25] in the USRP to wait for transmission at time  $T_{U,i} = t_E$ . If the USRP finds out that its current hardware time  $T_{U,i} > t_E$ , it will drop the packet and return a status “L” (which stands for Late [26]) to the PC and the transmission is considered to have failed. Our system needs to avoid such failures.

In our time-slotted system, packet transmission is challenging in two ways:

- a). the PC does not have direct access to the current *USRP Time*;
- b). there is an uncontrollable latency between the PC and the USRP.

In other words, the PC needs to estimate the *USRP Time* indirectly and prepare the packet in advance to compensate for the latency.

For issue (a), although the *Sample Counter* does not provide the current *USRP Time*, it provides the most updated *USRP Time on PC*. When the PC calls a function provided by the *Sample Counter* to get the *USRP Time*, it returns the latest number of samples that have passed through it. In other words, the value returned by the *Sample Counter* represents the time of the latest sample coming from the USRP, which only experiences the delay between the PC and the USRP, and the value is

$$T_{UP,i} = T_{U,i} - \delta_{RX,i}, \quad (12)$$

where  $\delta_{RX,i}$  is RX delay between PC and USRP in IoT device  $i$ .

For issue (b), an illustration is shown in Fig. 6, where  $\delta_{TX,0}$  and  $\delta_{TX,i}$  are the PC-USRP delays at the AP and IoT device  $i$ , respectively. If the PC of a node does not take the delay into consideration and sends a packet to the USRP at *USRP Time*  $T_{U,i} = t_E$  with the timestamp  $t_E$ , when the packet arrives at the USRP hardware, *USRP Time* is already  $T_{U,i} = t_E + \delta_{TX,i}$ . Therefore, the PC of node  $i$  needs to make sure the packet is sent to the *SampleQueue* at least  $\delta_{TX,i}$  in advance.

A straightforward solution is to let the PC intentionally prepare the packet content and its timestamp far before the targeted transmission time. For example, when a beacon arrives at the node's PC, the node immediately prepares the packets to be transmitted  $K$  time frames later where  $K \gg 1$  and sends these packets to the USRP. However, this method is not viable for most time-sensitive IIoT applications. This is because if the packet is prepared far before its transmission time, say  $t_E = t_{UP,i} + K \cdot T_{Frame}$ , where  $T_{Frame}$  is the duration of a time frame, the end-to-end delay of the packet will become excessive.

To achieve low latency transmission, all unnecessary overhead delay should be removed before the packet transmission. For a time-slotted multiuser system, each IoT device can only transmit its packets at its pre-allocated time slots. Taking issues (1) no direct access to *USRP time* and (2) uncontrollable latency between PC and USRP into consideration, the timing for sending packets from PC to USRP needs to be carefully set. In the following, we propose an effective mechanism to deal with this issue.

#### A. Wake-ahead-a-bit transmission scheme

To prevent the PC from generating and sending a packet to the USRP too much ahead of its transmission time, we put forth a scheme called “Wake-ahead-a-bit”. In essence, the PC generates and sends packets based on an estimated

transmission delay. For a packet to be transmitted in the time slot  $j$  of frame  $k$  by node  $i$ , it needs to be sent by the PC at

$$t_{UP,i} = s_{i,j}^k - \delta_{TX,i}, \quad (13)$$

where  $\delta_{TX,i}$  is the delay from the PC to the USRP. Combining (12) and (13), we know that node  $i$ 's PC needs to send the packet to the USRP on or before

$$t'_{UP,i} = s_{i,j}^k - \delta_{TX,i} - \delta_{RX,i} = s_{i,j}^k - \delta_{RTT,i}, \quad (14)$$

where  $\delta_{RTT,i}$  is the estimated round-trip time (RTT) between the PC and the USRP hardware of the  $i$ -th node. The question then becomes how to estimate the RTT. Fortunately, a simple tool can be used to obtain the latency between the PC and the USRP: *PING test*. Internet Control Message Protocol (ICMP) packets, which are sent by the *ping* command on the PC, go through the Ethernet to reach the USRP, and the USRP will give ICMP response packets back to the PC.

Because the RTT between the PC and the USRP has large jitters, safety margins need to be added. We follow how the TCP adds safety margin to handle possible jitters in setting the RTO [27]. In particular, the safety margin for the  $i$ -th node is calculated by

$$\omega_i = \beta \cdot \sigma_{RTT,i}, \quad (15)$$

where  $\beta$  is an adjustable coefficient and  $\sigma_{RTT,i}$  is the measured deviation of the RTT of the  $i$ -th node. Consequentially, the packet targeted at the  $j$ -th time slot should be sent by the  $i$ -th node's PC at

$$t''_{UP,i} = s_{i,j}^k - \delta_{RTT,i} - \beta \cdot \sigma_{RTT,i}. \quad (16)$$

From this point, the algorithm becomes simple. We define  $T_{adv}$  to be the time for the PC to “wake ahead”, and we have

$$T_{adv} = \delta_{RTT,i} + \beta \cdot \sigma_{RTT,i}. \quad (17)$$

If node  $i$  wants to transmit a packet in slot  $j$  of frame  $k$ , we set the transmission thread<sup>4</sup> to the sleep status and then set a countdown timer to count with the initial value  $s_{i,j}^k - T_{adv}$ .

When the timer counts to zero, the thread wakes up, prepares the packet content, tags the timestamp  $s_{i,j}^k$  to the packets and sends them to the *SampleQueue* in the USRP. After that, the timer will be reset to  $s_{i,j'}^{k'} - T_{adv}$  again with  $j'$  and  $k' \geq k$ , where  $(j', k')$  is the slot for the next transmission. A flowchart is provided in Fig. 8 to show the procedures of the algorithm.

#### B. Implication of Wake-ahead-a-bit algorithm

For a wireless IoT network that leverages the *Wake-ahead-a-bit* algorithm, it needs to let its AP/IoT devices' applications to generate packet(s)  $T_{adv}$  ahead of the USRP transmission time. Taking the wireless sensor network as an example, if its application is a sensor sensing data, the sensor will takes a measurement and report it at time  $T_{adv}$  ahead of the transmission time. The return packet from the AP could be

<sup>4</sup>GNURadio is a thread-based program which separates the processing of packets into many threads. The packet preparation and transmission in GNURadio on the PC runs on a thread while the reception of packets runs on another thread.

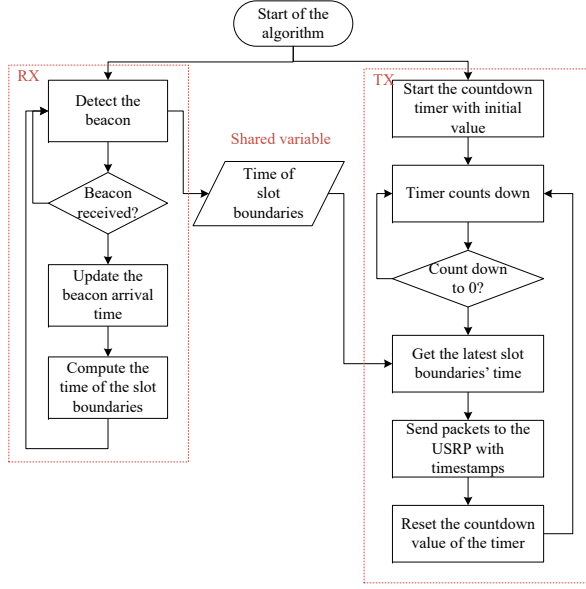


Fig. 8. The flowchart of the wake-ahead-a-bit algorithm.



Fig. 9. The testbed of our experiment. Three sets of Powerful PC + USRP in an indoor office environment. One of them serves as the AP and the other two are the IoT devices.

a packet generated by a controller based on the sensed data. Thus, by using the minimum acceptable  $T_{adv}$ , the *Wake-ahead-a-bit* algorithm can reduce the round-trip delay of a feedback loop in a control system.

## V. EXPERIMENTAL VALIDATION

To evaluate RTTS-SDR, we deployed three sets of USRP X310 with onboard TCXO and UBX-160 daughterboards [28] (i.e., there are three nodes, one of which is the AP) (see Fig. 9). Each of the USRP is connected to a PC with a 10Gbps Ethernet cable. The PC is equipped with a 16-core AMD 1950X Processor 3.4GHz and 64G RAM. The operating system is Ubuntu 16.04 LTS with kernel version 4.15.0-60-generic, installed with UHD 3.9.7 and GNURadio 3.7.11.

The PHY-layer adopts the settings as shown in TABLE I. The number of time slots in each time frame is set to 19, including the beacon. Three nodes transmit in a round-robin manner. That is, the time slot of each of the nodes

TABLE I  
PARAMETERS OF THE PHY-LAYER IN THE EXPERIMENT

Center frequency	2.418GHz
Bandwidth	10MHz
Length of payload	128 OFDM symbols
Modulation	BPSK
Channel code	1/2 convolutional code
Length of preamble	4 OFDM symbols
Length of cyclic-prefix	16
Guard time	360 samples

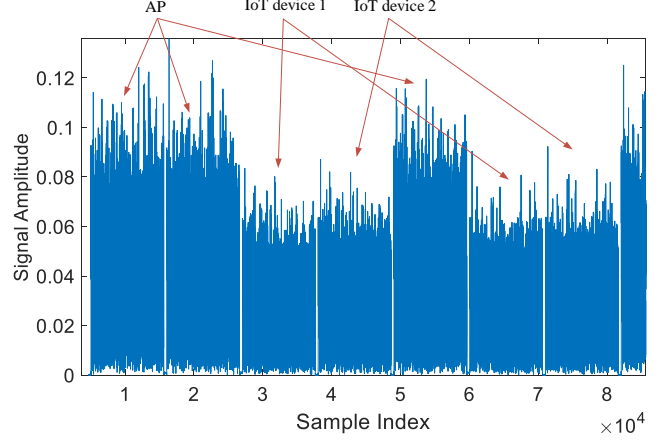


Fig. 10. An example of round-robin TDMA implemented on RTTS-SDR. We can see visually that the time-slot boundaries of different nodes are synchronized.

is pre-assigned. To clearly show the structure of time slots and the gaps between two slots, we adopt the durations of 360 samples as the guard time between two consecutive slots. We emphasize that in actual system, this excessive number of samples for the guard time is not necessary. It is purely an artificial setting so that we can visually delineate the different time slots in Fig. 10.

### A. Usability of the time-slotted system

We ran the system in an office environment. We captured the signal at the receiver side of the AP. The transmit power of three nodes are intentionally not carefully calibrated to better emulate practical scenarios.

As shown in Fig. 10, the first time slot is a beacon, followed by round robin transmissions of data packets from all three nodes, including the AP. Note that the round-robin transmission scheme is just an example which can be changed based on the traffic requirements. The changes can also be done in real-time by the AP through embedding the scheduling changes in the beacon (i.e., beacons, besides serving as a timing reference, also contain instructions from the AP).

### B. Accuracy of synchronization

We next tested the accuracy of our synchronization algorithm. We first measured the clock drift between the IoT device 1 and the AP in the absence of synchronization. To do so, we compared the timestamps of received beacons and the expected



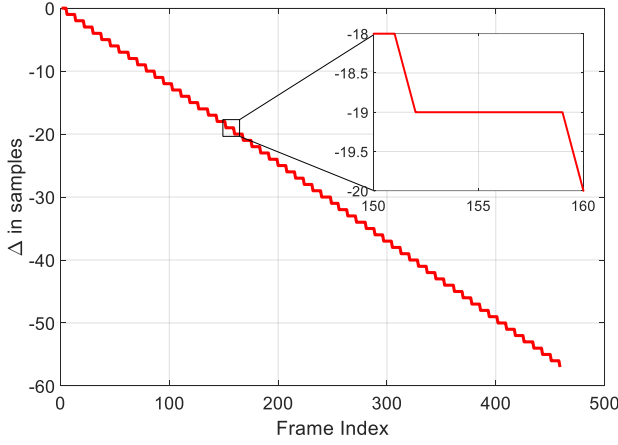


Fig. 11. Clock drift  $\Delta$  (in units of number samples) between the AP node and one of the IoT devices.

timestamps of the same beacons at the IoT device 1. The expected timestamp of the beacon in frame  $k$  is

$$t_{\text{Beacon}}^k = t_{\text{Beacon}}^0 + kNT_s. \quad (18)$$

On the other hand, the actual timestamp of the received beacon in frame  $k$  is  $\tilde{t}_{\text{Beacon}}^k$ . Therefore, the clock drift at frame  $k$  of the IoT device 1 can be defined as

$$\Delta t_{\text{Beacon}}^k = t_{\text{Beacon}}^k - \tilde{t}_{\text{Beacon}}^k. \quad (19)$$

Fig. 11 shows the clock drift in terms of samples. The duration of one time slot is

$$T_s = [(128 + 4) \times (64 + 16) + 360] \cdot T_{\text{sample}} \\ = 10920 \times \frac{1}{10 \times 10^6} = 1.092 \text{ ms} \quad (20)$$

Recall that there are 19 time slots in one time frame in our experiment, the duration of one time frame is thus  $1.092 \times 19 = 20.748 \text{ ms}$ . As shown in Fig. 11, the clocks of two nodes drift apart by more than 5 samples after 1 second (i.e., 48.197 frames). After 400 frames, the clock drift increases to 50 samples. Even disregarding the propagation time and considering only the clock drift, the guard time  $T_{\text{Guard}} = 360T_{\text{sample}}$  can only tolerate around 2880 frames. In other words, in about one minute at most, the transmissions from two nodes in two consecutive slots will collide with each other if we do not have the time-slot alignment procedure. The curve in Fig. 11 is staircase-like since the clocks drift apart by less than one sample between two consecutive frames: they drift apart by one sample after a few frames. From the result, we can also conclude that when synchronization is turned on, and if an IoT device misses the detections of a few successive beacons and cannot perform synchronization for the few successive frames, the alignment of its slot boundaries will still be within one sample (about 1 sample drift every 7 frames in the lack of synchronization).

To measure the accuracy of our synchronization algorithm, we analyze the timing of the received signals at the AP. Specifically, since the USRP clock of the AP is used as the reference clock, and the AP's RX path provides a timestamp for each of the received packets (includes its own packets), the timestamp can be used to measure each node's synchrony.

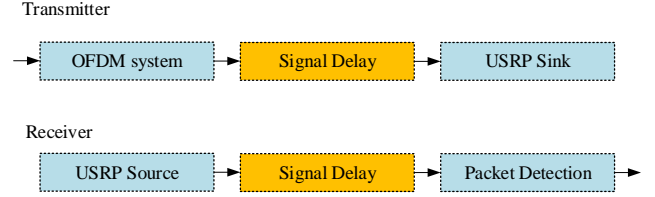


Fig. 12. The locations of adding the Signal Delay block in the GNURadio TX and RX paths of the IoT devices.

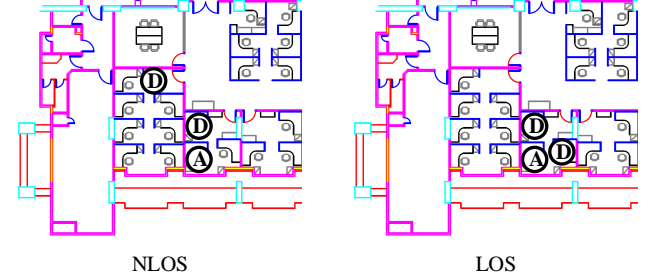


Fig. 13. The deployed locations of three sets of PC+USRP in LOS and NLOS. A is the AP and D are the IoT devices.

Let  $\tilde{R}_{i,j}^k$  be the actual timestamp of the received packet sent from node  $i$  in the  $k$ -th frame's slot  $j$  and  $R_{i,j}^k$  be the corresponding expected timestamp. The absolute difference of two timestamps  $\Delta R_{i,j}^k = |R_{i,j}^k - \tilde{R}_{i,j}^k|$  is used as the metric to quantify the synchrony between the AP and the IoT device  $i$ .

To evaluate  $\Delta R_{i,j}^k$  with non-negligible propagation delays, we emulated a 90-meter propagation path between the AP and one of the IoT devices (IoT device 1) and a 30-meter propagation path between the AP and another IoT device (IoT device 2). The emulation was done by inserting signal delay blocks [29] in the GNURadio TX paths and RX paths of the IoT devices to delay the incoming and outgoing signals (see Fig. 12). Specifically, the signal delay blocks in the GNURadio TX paths emulate the propagation delays  $d_{i,0}$  and the delay blocks in the GNURadio RX paths emulate  $d_{0,i}$ . No modification was done in the AP's flowgraph. For comparison, we also investigated the performance of the scheme that does not compensate for the propagation delay. To evaluate the robustness of the synchronization algorithm, the above experiments were carried out in Line-of-Sight (LoS) as well as Non-Line-of-Sight (NLoS) environments. For the Non-Line-of-Sight environment, we put the AP and IoT devices in different rooms where there is a wall blocking the direct paths between them (see Fig. 13).

Ten rounds of tests with  $10^3$  frames per round were run in each case. The results are shown in Fig. 14. Note that the resolution of our misalignment measurement is 1 sample ( $0.1 \mu\text{s}$ ). Thus, a measured misalignment of 0 corresponds to misalignment of  $-0.5$  to  $+0.5$  samples and a measured misalignment of 1 corresponds to misalignment of  $-1.5$  to  $-0.5$  or  $0.5$  to  $1.5$  samples. Fig. 14 shows that our system can align the slot boundaries to within  $\pm 0.5$  samples 90% of the time and to within  $\pm 1.5$  samples 100% of the time for both LoS and NLoS environments. If the emulated propagation delay is

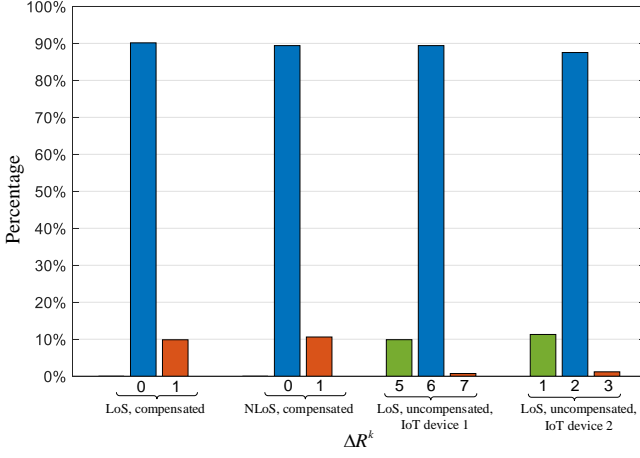


Fig. 14. The percentage of achieved  $\Delta R^k$  in the system in three different cases. All three cases have the same setting of propagation delays  $d_{0,1} = d_{1,0} = 3 \times 10^{-7}s$ ,  $d_{0,2} = d_{2,0} = 1 \times 10^{-7}s$ . The x-axis is the absolute difference of the actual timestamps and the expected timestamps  $\Delta R^k$ , and the y-axis is the percentage of that value for  $\Delta R^k$ .

not compensated, on the other hand, additional misalignment corresponding to the uncompensated round-trip delay will be introduced.

### C. Latency of packet delivery

To demonstrate the benefits of our “Wake-ahead-a-bit” algorithm, we performed tests to measure end-to-end latency. Specifically, we measured the round-trip time of an IoT device delivering a packet to the AP followed by the AP delivering a packet back to the IoT device. Just before preparing a packet for transmission, the IoT device marks down its PC time as the packet’s transmission PC time  $t_{P-TX}$ . After the AP’s PC receives and decodes the packets, it prepares a feedback packet and sends it back to the IoT device. When the IoT device receives the feedback packet from the AP, it checks the transmission PC Time  $t_{P-RX}$  of the packet and compute the round-trip time by  $t_{RTT} = t_{P-RX} - t_{P-TX}$ .

Before running the tests, we measured the RTT between PC and the USRP of the IoT device  $i$ , i.e.  $\delta_{RTT,i}$ , by running the “PING” test. Because the raw samples were transmitted between PC and the USRP with bursty transmission, we let the PING test ran in a bursty way. The PING test was done for 10 rounds, and in each round we sent 1000 packets with the transmission interval equals to  $1ms$ . The PING test shows that the mean RTT,  $\delta_{RTT,i}$ , is  $1.154ms$  and the deviation,  $\sigma_{RTT,i}$ , is  $0.812ms$ . Therefore, the time we should send in advance based on (16) can be set to be  $2ms$ , assuming  $\beta = 1$  and a small amount of added time for packet preparation.

Again,  $T_{adv}$  is the time for the PC to “wake ahead”. For our “Wake-ahead-a-bit” algorithm, we set  $T_{adv} = 2ms$ . For benchmarking, we also ran the tests with  $T_{adv} = 10ms$  which is approximately half the duration of a frame, and  $T_{adv} = 20ms$ , which is approximately the duration of a frame. Each test consists of  $10^6$  pairs of packets between the IoT device and the AP. Based on the statistics of these packet, we obtain the 99-percentile and 99.99-percentile RTT.

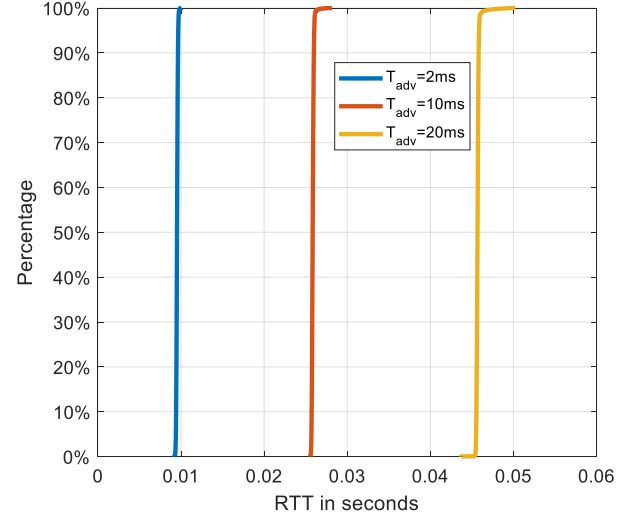


Fig. 15. The RTT of delivering a packet with different  $T_{adv}$ .

As shown in Fig. 15,  $T_{RTT}$  depends significantly on  $T_{adv}$ . For  $T_{adv} = 2ms$ , the 99-percentile RTT is  $9.97ms$  and the 99.99-percentile RTT is  $10.39ms$ . For  $T_{adv} = 10ms$ , the 99-percentile RTT is  $26.16ms$  and the 99.99-percentile RTT is  $27.49ms$ . And for  $T_{adv} = 20ms$ , the 99-percentile RTT is  $46.19ms$  and the 99.99-percentile is  $49.28ms$ .

We further explored the  $T_{RTT}$  of short packets. IoT applications with low-latency requirements typically need to transmit very little data. Thanks to the reconfigurability of RTTS-SDR (see Appendix A), we could easily reduce the number of OFDM symbols in a packet from 128 to 12. The PHY-layer uses BPSK modulation and 1/2 convolutional code, giving a packet length of 36 bytes, which is close to the packet size of 32 bytes defined in 5G for ultra-reliable low-latency communication (URLLC) [30]. The guard time between two consecutive slots is also reduced from 360 samples to 80 samples. We set  $T_{adv}$  to  $2ms$ . To explore the 99.9999-percentile RTT, we ran the tests with  $10^7$  pairs of short packets between the IoT device and the AP. As shown in Fig. 16, the 99-percentile RTT is  $6.90ms$ , the 99.99-percentile RTT is  $7.24ms$ , and the 99.9999-percentile RTT is  $7.37ms$ . Indeed, the RTTs of all packets are bounded by  $7.5ms$ . This implies that the one-way delay is bounded by  $3.75ms$ .

In the context of a control system in which the controller is connected to the AP and the sensor and the actuator are connected to the IoT device, the above round-trip delay corresponds to the feedback-loop delay of the control system. Our system can guarantee a feedback loop delay bounded by  $7.5ms$ .

## VI. CONCLUSIONS

This paper puts forth a real-time time-slotted system on the USRP-SDR platform for time-sensitive wireless networks. Specifically, we proposed two new techniques to handle the issues raised by the latency between the PC and the USRP: (i) sample counting in the receive path for time-slot synchronization; (ii) Wake-ahead-a-bit algorithm to time the forwarding of a packet from the PC to the USRP in the transmit path

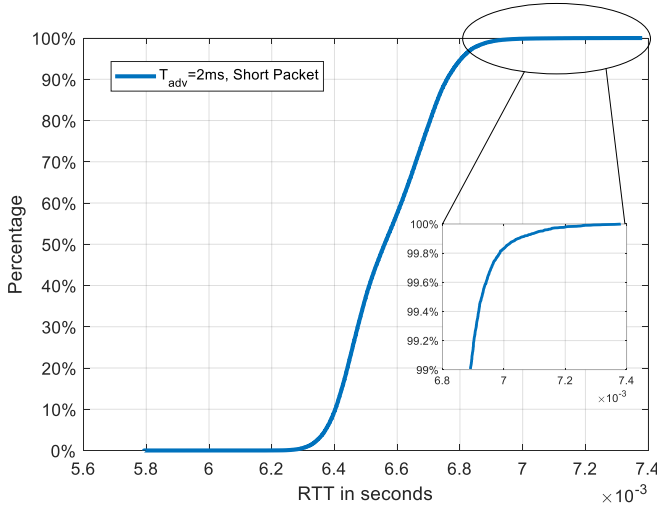


Fig. 16. The RTT of delivering a short packet with  $T_{adv} = 2ms$ .

to achieve low latency. With these techniques, the system can achieve sub-microsecond time synchronization ( $100ns$ ) among nodes and 3.75-ms end-to-end delay. Overall, our system can fulfill part of the URLLC defined in 5G (e.g., medium-voltage electric power distribution grid, augmented reality, and mobile panel control panels with safety functions [31, pp.159]). It demonstrates the viability of building the time-sensitive wireless IoT networks on the SDR platform.

#### APPENDIX RECONFIGURABILITY<sup>5</sup>

Many of the parameters in the PHY-layer of RTTS-SDR are reconfigurable. Specifically, the following parameters can be changed easily in our system: (1) Subcarrier mapping in the OFDM modulation and demodulation; (2) Length of the cyclic prefix (CP); and (3) Packet length; and (4) Bitrates. In this appendix, we briefly introduce how the system provides support to each of the reconfigurable parameters.

**Subcarrier mapping.** A changeable subcarrier mapping allows the system to fit into wireless channels of different spectrum characteristics. For example, when the unused spectrum is discontinuous, the system can disable some of its subcarriers so that it will not interfere with other existing wireless systems that already occupy the used spectrum of those subcarriers. Meanwhile, STS and LTS are also adjusted so that there is no out-of-band signal. Packet detection algorithm, which has been modified to be generic, is capable of detection any kind of subcarrier mapping.

**Length of OFDM CP.** The length of CP is an essential parameter for the scenarios where the delay spread is a big concern. For our time-slotted system, the length of CP  $N_{CP}$  can be varying from 0 to the length of FFT/IFFT  $N_{FFT}$ . Note that the CP may be a large overhead if a system is set with a large  $N_{CP}$  but runs in a small-delay-spread environment. The

<sup>5</sup>Readers who are interested in the software code of RTTS-SDR can send a request to [32]. We have attempted to make RTTS-SDR reconfigurable for other systems than the TDMA system described in this paper, and we are interested in feedback from users who would like to try out RTTS-SDR.

required CP length depends on the coverage of the system to be prototyped.

**Packet length.** The length of packets in a system determines the major scope of applications of that system. Our system supports packet lengths starting from 0 (no payload) to any positive value.

**Bitrates.** Our system supports all the bitrates in 802.11a/g/n and it is also capable of changing the bitrate packet-by-packet. Users can easily change the bitrate of a packet by giving different parameters to the API.

#### REFERENCES

- [1] G. Brown, "Ultra-reliable low-latency 5g for industrial automation," p. 11. [Online]. Available: <https://www.qualcomm.com/media/documents/files/read-the-white-paper-by-heavy-reading.pdf>
- [2] S. Melnyk, A. G. Tesfay, K. Alam, H. D. Schotten, V. Sark, N. Maletic, M. Ramadan, M. Ehrig, T. Augustin, N. Franch, and G. Fettweis, "Reliable low latency wireless communication enabling industrial mobile control and safety applications." [Online]. Available: <http://arxiv.org/abs/1804.07553>
- [3] Y. Liao, E. de Freitas Rocha Loures, and F. Deschamps, "Industrial internet of things: A systematic literature review and insights," *IEEE Internet of Things Journal*, vol. 5, no. 6, pp. 4515–4525, 2018.
- [4] "Everything you need to know about the industrial internet of things." [Online]. Available: <https://www.ge.com/digital/blog/everything-you-need-know-about-industrial-internet-things2>
- [5] V. K. L. Huang, Z. Pang, C. A. Chen, and K. F. Tsang, "New trends in the practical deployment of industrial wireless: From noncritical to critical use cases," *IEEE Industrial Electronics Magazine*, vol. 12, no. 2, pp. 50–58, June 2018.
- [6] H. Hellstrom, M. Luvisotto, R. Jansson, and Z. Pang, "Software-defined wireless communication for industrial control: A realistic approach," *IEEE Industrial Electronics Magazine*, vol. 13, no. 4, pp. 31–37, Dec 2019.
- [7] M. Luvisotto, Z. Pang, and D. Dzung, "Ultra high performance wireless control for critical applications: Challenges and directions," *IEEE Transactions on Industrial Informatics*, vol. 13, no. 3, pp. 1448–1459, 2016.
- [8] H. Chen, R. Abbas, P. Cheng, M. Shirvanimoghaddam, W. Hardjawana, W. Bao, Y. Li, and B. Vucetic, "Ultra-reliable low latency cellular networks: Use cases, challenges and approaches," *IEEE Communications Magazine*, vol. 56, no. 12, pp. 119–125, December 2018.
- [9] F. K. Jondral, "Software-defined radio's basics and evolution to cognitive radio," *EURASIP Journal on wireless communications and networking*, vol. 2005, no. 3, p. 652784, 2005.
- [10] B. Bloessl, C. Leitner, F. Dressler, and C. Sommer, "A gnu radio-based ieee 802.15. 4 testbed," *12. GI/ITG KuVS Fachgespräch Drahtlose Sensornetze (FGSN 2013)*, pp. 37–40, 2013.
- [11] K. Tan, H. Liu, J. Zhang, Y. Zhang, J. Fang, and G. M. Voelker, "Sora: high-performance software radio using general-purpose multi-core processors," *Communications of the ACM*, vol. 54, no. 1, pp. 99–107, 2011.
- [12] B. Drozdenko, M. Zimmermann, T. Dao, K. Chowdhury, and M. Leeser, "Hardware-software codesign of wireless transceivers on zynq heterogeneous systems," *IEEE Transactions on Emerging Topics in Computing*, vol. 6, no. 4, pp. 566–578, 2017.
- [13] H. Wu, T. Wang, Z. Yuan, C. Peng, Z. Li, Z. Tan, B. Ding, X. Li, Y. Li, J. Liu *et al.*, "The tick programmable low-latency sdr system," in *Proceedings of the 23rd Annual International Conference on Mobile Computing and Networking*, 2017, pp. 101–113.
- [14] R. Torrego, I. Val, E. Muxika, E. Muxika, X. Iturbe, and K. Benkrid, "Data coding functions for software defined radios implemented on r3tos," in *22nd International Conference on Field Programmable Logic and Applications (FPL)*. IEEE, 2012, pp. 33–40.
- [15] "Membership ORAN alliance." [Online]. Available: <https://www.o-ran.org/membership>
- [16] M. Luvisotto, Z. Pang, D. Dzung, M. Zhan, and X. Jiang, "Physical layer design of high-performance wireless transmission for critical control applications," *IEEE Transactions on Industrial Informatics*, vol. 13, no. 6, pp. 2844–2854, 2017.

- [17] N. Choudhury, R. Matam, M. Mukherjee, and J. Lloret, "Lbs: A beacon synchronization scheme with higher schedulability for iee 802.15.4 cluster-tree-based iot applications," *IEEE Internet of Things Journal*, vol. 6, no. 5, pp. 8883–8896, 2019.
- [18] T. Xu, C. Masouros, and I. Darwazeh, "Waveform and space precoding for next generation downlink narrowband iot," *IEEE Internet of Things Journal*, vol. 6, no. 3, pp. 5097–5107, 2019.
- [19] —, "Design and prototyping of hybrid analogdigital multiuser mimo beamforming for nonorthogonal signals," *IEEE Internet of Things Journal*, vol. 7, no. 3, pp. 1872–1883, 2020.
- [20] "TUNTAP documentation." [Online]. Available: <https://www.kernel.org/doc/Documentation/networking/tuntap.txt>
- [21] "Stream tags in gnu radio." [Online]. Available: [https://wiki.gnuradio.org/index.php/Stream\\_Tags](https://wiki.gnuradio.org/index.php/Stream_Tags)
- [22] E. Research, "Uhd (usrp hardware driver)." [Online]. Available: <https://www.ettus.com/sdr-software/uhd-usrp-hardware-driver/>
- [23] "IEEE standard for a precision clock synchronization protocol for networked measurement and control systems," *IEEE Std 1588-2008 (Revision of IEEE Std 1588-2002)*, pp. 1–300, 2008.
- [24] B. Bloessl, M. Segata, C. Sommer, and F. Dressler, "An iee 802.11a/g/p ofdm receiver for gnu radio," in *Proceedings of the Second Workshop on Software Radio Implementation Forum*, ser. SRIF 13. New York, NY, USA: Association for Computing Machinery, 2013, pp. 9–16. [Online]. Available: <https://doi.org/10.1145/2491246.2491248>
- [25] "Synchronizing USRP events using timed commands in uhd." [Online]. Available: [https://kb.ettus.com/Synchronizing\\_USRP\\_Events\\_Using\\_Timed\\_Commands\\_in\\_UHD](https://kb.ettus.com/Synchronizing_USRP_Events_Using_Timed_Commands_in_UHD)
- [26] "Troubleshooting performance issues." [Online]. Available: [https://files.ettus.com/manual/page\\_usrp\\_x3x0\\_config.html#x3x0cfg\\_hosthw\\_troubleshooting](https://files.ettus.com/manual/page_usrp_x3x0_config.html#x3x0cfg_hosthw_troubleshooting)
- [27] G. A. Leon and I. Widjaja, *Communication networks: fundamental concepts and key architectures*. MacGraw-Hill, 2004.
- [28] "USRP X310 specs." [Online]. Available: [https://kb.ettus.com/X300/X310#X310\\_2](https://kb.ettus.com/X300/X310#X310_2)
- [29] "Signal delay blocks documentation." [Online]. Available: [https://www.gnuradio.org/doc/doxygen/classgr\\_1\\_1blocks\\_1\\_1delay.html](https://www.gnuradio.org/doc/doxygen/classgr_1_1blocks_1_1delay.html)
- [30] 3GPP, "Study on Scenarios and Requirements for Next Generation Access Technologies," 3rd Generation Partnership Project (3GPP), Technical Specification (TS) 38.913, June 2017, version 14.3.0.
- [31] —, "Study on Communication for Automation in Vertical Domains (Release 16) ," 3rd Generation Partnership Project (3GPP), Technical Report (TR) 22.804, Sept 2018, version 16.1.0.
- [32] "Source code for RTTS-SDR." [Online]. Available: <http://wireless.ie.cuhk.edu.hk/rtts-sdr.html>